

Studies of ion energy and yield from argon clusters heated by intense femtosecond laser pulses

S.H. Li^{1,2,a}, C. Wang², J.S. Liu², X.X. Wang², R.X. Li², G.Q. Ni², and Z.Z. Xu²

¹ Department of Physics, Shantou University, Shantou 515063, P.R. China

² Laboratory for High Intensity Optics, Shanghai Institute of Optics and Fine Mechanics, Chinese Academy of Sciences, Shanghai 201800, P.R. China

Received 6 September 2004

Published online 13 July 2005 – © EDP Sciences, Società Italiana di Fisica, Springer-Verlag 2005

Abstract. Using time-of-flight spectrometry, the interaction of intense femtosecond laser pulses with argon clusters has been studied by measuring the energy and yield of emitted ions. With two different supersonic nozzles, the dependence of average ion energy \bar{E} on cluster size \bar{n} in a large range of $\bar{n} \approx 3 \times 10^3 \sim 3 \times 10^6$ has been measured. The experimental results indicate that when the cluster size $\bar{n} \leq 3 \times 10^5$, the average ion energy $\bar{E} \propto \bar{n}^{0.5}$, Coulomb explosion is the dominant expansion mechanism. Beyond this size, the average ion energy gets saturated gradually, the clusters exhibit a mixed Coulomb-hydrodynamic expansion behavior. We also find that with the increasing gas backing pressure, there is a maximum ion yield, the ion yield decreases as the gas backing pressure is further increased.

PACS. 36.40.Gk Plasma and collective effects in clusters – 52.50.Jm Plasma production and heating by laser beams (laser-foil, laser-cluster, etc.)

1 Introduction

In the past decade intense laser interaction with van der Waals-bonded clusters received remarkable attention, many research groups have reported that these interactions can be very energetic. Studies on the interaction of a cluster target with laser pulses have shown that X-ray emission in keV range [1] is generated, MeV ions [2] and multi-keV electrons [3] are ejected from large clusters, laser driven table-top nuclear fusion [4] has also been realized.

Several theoretical models [5, 6] have been developed to account for these observations of the intense laser interaction with clusters. “Hydrodynamic expansion” model [5] treats the expanding cluster as a spherical uniform microplasma. Multiple ionization of argon atoms inside the cluster proceeds at the leading edge of the laser pulse (so-called inner ionization), after a part of the initially ionized electrons is removed from the cluster by the laser field (so-called outer ionization), most of the electrons are retained in the cluster due to the charge buildup of positive ions. The retained electrons absorb the laser energy via inverse bremsstrahlung and the cluster expands mainly due to the hydrodynamic force. The “ionization ignition-Coulomb explosion” model [6] predicts an avalanche ionization in a cluster due to the combined fields of the laser and the ionized cluster atoms, most of the ionized elec-

trons leave the cluster and the buildup of positive charge results in the explosion of the cluster due to the Coulombic repulsion of the ions. It is generally believed that the expansion mechanism of small clusters is Coulomb explosion. For argon clusters, with the utilization of magnetic deflection time-of-flight mass spectrometry, Lezius et al. [7] found that Coulomb explosion is the main mechanism of the cluster expansion in the range of the cluster size $\bar{n} \leq 1.8 \times 10^5$ (if using the same scaling law of cluster size in our paper, the above cluster size range is $\bar{n} \leq 5.5 \times 10^4$).

In this paper, by using two nozzles with different diameters and half opening angles, we have measured the dependence of the average energy of argon ions on cluster size in a large range of $\bar{n} \approx 3 \times 10^3 \sim 3 \times 10^6$. The experimental results indicate that when $\bar{n} \leq 3 \times 10^5$, the average ion energy $\bar{E} \propto \bar{n}^{0.5}$, Coulomb explosion is believed to be the main mechanism of the cluster expansion. Beyond this size, it is the result of common effect of both the Coulomb repulsion force and the hydrodynamic force.

2 Experimental method

Our experimental setup is similar to that described elsewhere [8]. Briefly, the clusters are produced by supersonic expansion of argon gas into vacuum through a conical nozzle. The laser used is a chirped pulse amplification Ti:sapphire laser which delivers 60 fs pulses at the wavelength of 790 nm with a 10 Hz repetition rate. The laser

^a e-mail: shli@stu.edu.cn

light is focused using an off-axis parabolic mirror with the focal length of 20 cm and the laser intensity at the focal spot 2 mm downstream from the nozzle is about 2×10^{16} W/cm². The ions expelled from the clusters with velocities perpendicular to both the cluster jet and the laser beam propagated along a 120 cm field-free flight tube after a skimmer and were detected by a dual microchannel plate detector (DMCP). The front plate of the DMCP was held at -1.5 kV and the back was grounded. A grounded metal mesh was placed 5 mm before the DMCP to ensure that the flight-tube was field free. The signal from the DMCP was recorded using a 500 MHz, 1 GS/s digital oscilloscope (LeCroy 9350AL) and averaged with 100 shots. The ion energies were determined by time-of-flight (TOF) measurements through $E = \frac{1}{2}m(l/t)^2$ (m is the ion mass, l is the length of the flight tube and t is the flight time) and the energy distribution $f(E)$ of the ions can be obtained by conversion of the TOF spectrum $f(t)$ via $f(E) = f(t)(dE/dt)^{-1}$. The average ion energy \bar{E} was computed from the energy distribution function $f(E)$ through $\bar{E} = \int E f(E) dE / \int f(E) dE$.

The estimation of the average cluster size \bar{n} has been made based on the scaling law [9] using the Hagen empirical parameter Γ^* [10],

$$\bar{n} = 100 \left(\frac{\Gamma^*}{1000} \right)^{1.8} \quad (1)$$

$$\Gamma^* = k \frac{P_0 [\text{mbar}]}{(T_0 [\text{K}])^{2.29}} \left(\frac{d [\mu\text{m}]}{\tan \alpha} \right)^{0.85} \quad (2)$$

where P_0 is the gas backing pressure, T_0 is the gas stagnation temperature, α is the half opening angle of the conical nozzle, d is the nozzle diameter, and k is the gas condensation constant determined by the gas species, for argon in our case, $k = 1700$. The usual way of varying the cluster size is to change the gas backing pressure, but due to the limitation of pump capability of the vacuum system, and we are not sure whether the scaling law is still valid for higher gas backing pressure, the variation of gas backing pressure is confined under 32 bar in our experiment. To further increase the range of cluster size, we choose to change the nozzle parameter (the half opening angle and the diameter). In our experiment, two nozzles A and B have been used, the diameter and half opening angle for nozzle A and B are $700 \mu\text{m} - 3.3^\circ$ and $300 \mu\text{m} - 5.2^\circ$, respectively. In the pressure range of $P_0 = 2 \sim 32$ bar, according to equations (1) and (2), the corresponding ranges of cluster size for nozzle A and B are $2 \times 10^4 \sim 3 \times 10^6$ and $3 \times 10^3 \sim 5 \times 10^5$, respectively. So, with the utilization of the two nozzles, the range of cluster size in this experiment can be extended to $3 \times 10^3 \sim 3 \times 10^6$.

3 Results and discussion

Figure 1a is the time-of-flight spectra of ions from laser irradiated argon clusters under gas backing pressure of 8 bar, and Figure 1b is the corresponding energy spectra.

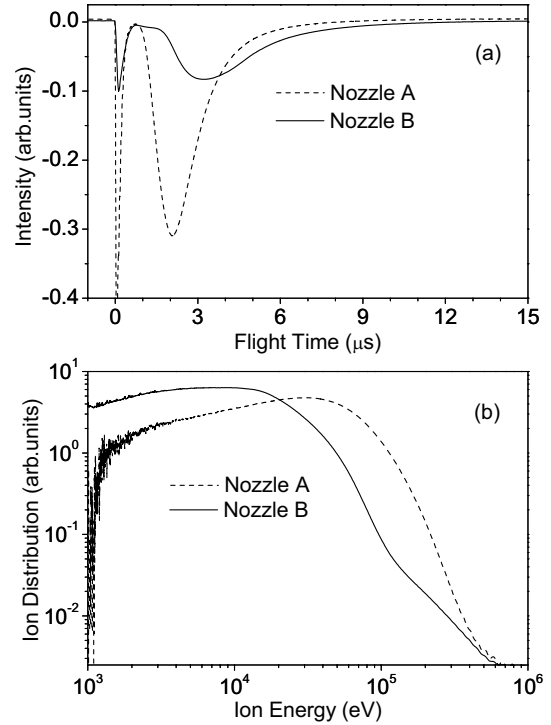


Fig. 1. Time-of-flight spectra of argon ions (a) and corresponding energy spectra (b) for nozzle A and B at backing pressure of 8 bar.

It can be seen that for nozzles A and B, through the gas backing pressures are the same, but due to the difference of cluster density and cluster size (the cluster sizes for nozzle A and B at 8 bar pressure are 4×10^4 and 2.8×10^5 atoms per cluster), there are much difference for the signal intensity and the energy distribution of the ions. The component of ions with higher energy for nozzle A is much greater than that of nozzle B. Contrary to it, the low energy ion component of nozzle A is much smaller than that of nozzle B. The average ion energies under the conditions are 60 and 27 keV, respectively.

In [11], the maximum ion energy was used by Sakabe et al. to characterize the laser-cluster interaction, if we adopt the maximum ion energy as in [11], there is no much difference of the maximum ion energies for the two different cluster sizes in Figure 1. Obviously, the average ion energy, rather than the maximum ion energy, could more reasonably reflect the correlation between the ion energy and the cluster size. Figure 2 shows the dependence of average ion energy on the cluster size in the range of cluster size from $3 \times 10^3 \sim 3 \times 10^6$ by using the two nozzles. We can see that the data correspond well in the overlapping range of cluster size of nozzles A and B. It not only indicates the validity of equations (1) and (2), but also reveals that when the laser parameters are kept unchanged, the average ion energy is determined by the cluster size.

In Figure 2, the variation of the average ion energy with cluster size can be divided into two ranges: when cluster size $\bar{n} \leq 3 \times 10^5$, the average ion energy \bar{E} and the cluster size \bar{n} approximately have the relation given

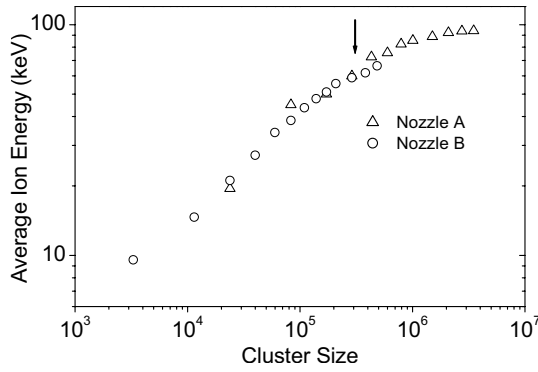


Fig. 2. Average ion energy as a function of cluster size.

by $\bar{E} \propto \bar{n}^{0.5}$, however, when $\bar{n} \geq 3 \times 10^5$, the average ion energy gets saturated gradually with increasing cluster size. As we have mentioned above, Lezius et al. found that the main expansion mechanism of argon cluster is Coulomb explosion for cluster size smaller than 5.5×10^4 . If the same relation between average ion energy and the cluster size represents the same expansion mechanism, the maximum cluster size of Coulomb explosion shown in [7] can then be extended to $\bar{n} \approx 3 \times 10^5$. The following simple analysis indicates that this postulation is reasonable.

When Coulomb explosion is the main expansion mechanism of a cluster, the average energy \bar{E} of ions emitted from the cluster is given by $\bar{E} \propto \bar{n} \langle Z \rangle^2 / r \propto \bar{n}^{2/3}$, here $\langle Z \rangle$ is the average charge state of the ions and r is the cluster radius at the end of outer ionization. This analysis is based upon two assumptions: (1) at a given laser intensity, the average charge state does not appreciably change with cluster size and (2) the cluster expansion is that the radius of the expanding cluster at the end of outer ionization is proportional to the initial radius. The extensive numerical simulations of cluster explosion made by Last et al. provide some justification for the validity of above assumptions [12]. The cluster size in the numerical simulations is basically less than 1000 atoms per cluster, however, for the case of larger cluster size here, the time needed for the realization of outer ionization will prolong with the increasing cluster size. At the end of the outer ionization, the ratio of the cluster radius with its original radius should increase with cluster size, if it satisfies $r/r_0 \propto \bar{n}^{1/6}$, then $\bar{E} \propto \bar{n}^{0.5}$, in accordance with our experimental result. It would be believed that the expansion mechanism of clusters up to $\bar{n} \approx 3 \times 10^5$ in size is Coulomb explosion. When $\bar{n} \geq 3 \times 10^5$, more electrons are confined in clusters, the expansion of the ions will ultimately reach a velocity given by the sound speed of the cluster plasma which is not sensitive to the cluster size [2], meaning that the ion energy will not change appreciably with cluster size, in agreement with our observation.

As shown in Figure 3, the dependence of the ion yield on gas backing pressure has also been measured. We find that there is an optimal gas backing pressure for the ion yield, and the optimal backing pressure for nozzle A and B is 10 and 18 bar, respectively. This phenomenon can be illustrated by the propagation and absorption effects

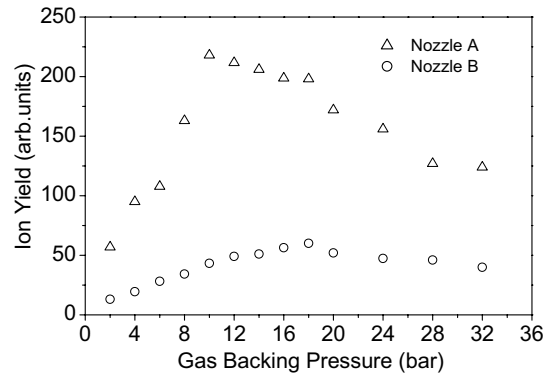


Fig. 3. Ion yield as a function of gas backing pressure.

of the laser pulse as it enters the cluster plume. The ion yield is mainly determined by the atom number in the focal area. When the gas backing pressure is low, the atom number is approximately proportional to the gas backing pressure, so, the ion yield increases with gas backing pressure accordingly. But as the gas backing pressure is further increased, a portion of the laser energy will be absorbed before reaching the focal spot. As a result, the plasma volume decreases, resulting in the decrease of the ion yield. For nozzle A, due to the plume density is larger than that of nozzle B under the same gas backing pressure, the absorption effect is stronger, so the optimal gas backing pressure related to the maximum ion yield is 10 bar, much less than 18 bar for nozzle B.

In laser-driven D-D fusion reaction, the neutron yield is mainly determined by the average energy and yield of the D ions, and a maximum neutron yield exists [13]. According to our experiment, we believe that with further optimization of the gas jet design and the use of a proper gas backing pressure, the neutron yield can be increased.

4 Conclusion

In conclusion, we have measured the dependence of average ion energy \bar{E} on cluster size \bar{n} in a large range of $\bar{n} \approx 3 \times 10^3 \sim 3 \times 10^6$. We find that when the cluster size $\bar{n} \leq 3 \times 10^5$, the average ion energy $\bar{E} \propto \bar{n}^{0.5}$, Coulomb repulsion force is the dominant expansion mechanism. Beyond this size, it is the result of common effect of both the Coulomb repulsion force and the hydrodynamic force. We also find that with the increasing of the gas backing pressure, there is a maximum ion yield and the yield decreases as the gas backing pressure is further increased.

This work was supported by the National Basic Research Special Foundation of China (No. G1999075200), and the National Natural Science Foundation of China (No. 60408008).

References

1. A. McPherson, B.D. Thompson, A.B. Borisov, K. Boyer, C.K. Rhodes, *Nature* **370**, 631 (1994)

2. T. Ditmire, J.W.G. Tisch, E. Spingate, M.B. Mason, N. Hay, R.A. Smith, J.P. Marangos, M.H.R. Hutchinson, *Nature* **386**, 54 (1997)
3. Y.L. Shao, T. Ditmire, J.W.G. Tisch, E. Springate, J.P. Marangos, M.H.R. Hutchinson, *Phys. Rev. Lett.* **77**, 3343 (1996)
4. T. Ditmire, J. Zweiback, V.P. Yanovsky, T.E. Cowan, G. Hays, K.B. Wharton, *Nature* **398**, 489 (1999)
5. T. Ditmire, T. Donnelly, A.M. Rubenchik, R.W. Falcone, M.D. Perry, *Phys. Rev. A* **53**, 3379 (1996)
6. C. Rose-Petruck, K.J. Schafer, K.R. Wilson, C.P.J. Barty, *Phys. Rev. A* **55**, 1182 (1997)
7. M. Lezius, S. Dobosz, D. Normand, M. Schmidt, *Phys. Rev. Lett.* **80**, 261 (1998)
8. S.H. Li, C. Wang, P.P. Zhu, X.X. Wang, R.X. Li, G.Q. Ni, Z.Z. Xu, *Chin. Phys. Lett.* **20**, 1247 (2003)
9. F. Dorchies, F. Blasco, T. Caillaud, J. Stevefeit, C. Stenz, A.S. Boldarev, V.A. Gasilov, *Phys. Rev. A* **68**, 023201 (2003)
10. O. F. Hagen, W. Obert, *J. Chem. Phys.* **56**, 1793 (1972)
11. S. Sakabe, S. Shimizu, M. Hashida, F. Sato, T. Tsuyukushi, K. Nishihara, S. Okihara, T. Kagawa, Y. Izawa, K. Imasaki, T. Iida, *Phys. Rev. A* **69**, 023203 (2004)
12. I. Last, J. Jorner, *Phys. Rev. A* **62**, 013201 (2000); *Phys. Rev. Lett.* **87**, 033401 (2001); *Phys. Rev. A* **64**, 063201 (2001)
13. J. Zweiback, R.A. Smith, T.E. Cowan, G. Hays, K.B. Wharton, V.P. Yanovsky, T. Ditmire, *Phys. Rev. Lett.* **84**, 2634 (2000)